ECCOMAS Congress 2016
VII European Congress on Computational Methods in Applied Sciences and Engineering
M. Papadrakakis, V. Papadopoulos, G. Stefanou, V. Plevris (eds.)
Crete Island, Greece, 5–10 June 2016

AN EXPERIMENTAL AND NUMERICAL STUDY ON THE PERFORMANCE OF AN INNOVATIVE VERTICAL-AXIS WIND TURBINE

Katarzyna Kludzinska[1], Krzysztof Tesch[1], and Piotr Doerffer[2]

[1]Fluid Mechanics Department
Gdansk University of Technology
ul. G. Narutowicza 11/12, 80-233 Gdansk, Poland
e-mail: kkludzinska@o2.pl

[2] Institute of Fluid Flow Machinery
ul. Fiszera 14, 80-231 Gdansk, Poland
e-mail: doerffer@imp.gda.pl

Keywords: Wind Turbines, Savonius wind turbine, CFD.

Abstract. *This paper introduces the innovative modification of the Savonius wind turbine being able to significantly increase efficiency in comparison with the classic design. This innovative design is equipped with a stator directing the flow. The presence of the stator increases the active surface area and generates higher torques acting on a shaft. Additionally, it makes it possible to take better advantage of wind energy and compensate the effect of larger active surface area. The larger the stator angle the higher the efficiency. One of the biggest problem of the classic design, namely its relatively low efficiency, is overcome.*

The results of an experimental investigation, carried out in the closed return wind tunnel, are presented for various conditions and configurations. These include the most important characteristic such as the torque and power coefficient as a function of the tip speed ratio. Furthermore, a three dimensional numerical analysis of the transient phenomena occurring in the innovative turbine is investigated. Evaluation and comparison criteria are proposed in order to evaluate and compare various designs and solutions. This makes it possible to explain the increased efficiency of the innovative design.

1 INTRODUCTION

The innovative vertical-axis wind turbine [2], shown in figure 1, is a modification of the Savonius classic design. It is equipped with an adjustable stator directing the flow and increasing the active surface area. This makes it possible to generate higher torques acting on a shaft and to take better advantage of wind energy and compensate the effect of larger active surface area. Thus one of the biggest problem of the classic design, namely its relatively low efficiency, is overcome.

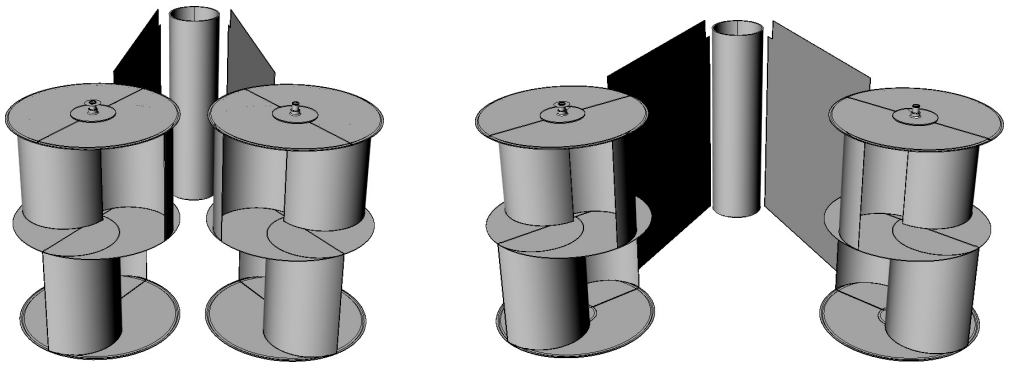

Figure 1: Innovative design.

The classic Savonius rotor has the simplest design of all devices converting wind into other energy forms. Despite numerous advantages, such as low noise, simplicity of design, applicability for a wide range of wind velocities, one of drawbacks of the classic design is its relatively low efficiency. It appears that the proposed modifications of Savonius like rotors in available literature have been developed using a trial and error method. This is because the flow structure inside the rotor is complicated and that is why in past investigations were limited only to laboratory tests [1, 6, 11, 10]. Recently attempts were made to analyse the structure of the flow through the Savonius rotor numerically [7, 9]. Most of data presented on the numerical aspect are mostly two-dimensional.

The main goal of this paper it to present results of an experimental investigation and to compare them with a three dimensional numerical analysis of the transient phenomena occurring in the innovative turbine. Furthermore, evaluation and comparison criteria are proposed in order to evaluate and compare various designs and solutions. An attempt to explain the increased efficiency of the innovative design has been also undertaken.

2 EXPERIMENTAL RESULTS

2.1 Coefficients

The most important characteristics of the wind turbines include the torque C_T and power C_P coefficients. Both of them are expressed as a function of the rotor tip speed ratio λ

$$\lambda = \frac{\omega D}{2\,U}. \tag{1}$$

The tip speed ration represents the ratio between the tangential speed of the tip of a blade and the velocity of the wind U. In the above definition ω stands for angular velocity and D is the diameter of the rotor.

The former of the mentioned non-dimensional quantities, i.e. C_T, is defined as

$$C_T = \frac{\bar{T}}{\frac{1}{4}\rho U^2 D^2 H} \tag{2}$$

where H is the rotor's height and ρ represents the density. For transient flows the average value of time dependent torque $T(t)$ is considered. This means that we deal with the distribution of C_T as a function of the angular position of the rotor α. The average value $\bar{T}$ is given by

$$\bar{T} = \frac{1}{\Delta t} \int_{t}^{t+\Delta t} T(t)\mathrm{d}t \tag{3}$$

where Δt stands for the time of one revolution. If the time step of the transient CFD calculations is constant we can approximate the integral average with the arithmetic average. The formal definition of the former non-dimensional quantity, i.e. power coefficient, is

$$C_P = \frac{\omega \bar{T}}{\frac{1}{2}\rho U^3 H D}. \tag{4}$$

Again, this is valid for transient flows, which is typical for the Savonius rotor operation. The non-dimensional quantities distributions as a function of λ are the basis for comparison the innovative design with the traditional solution or other studies.

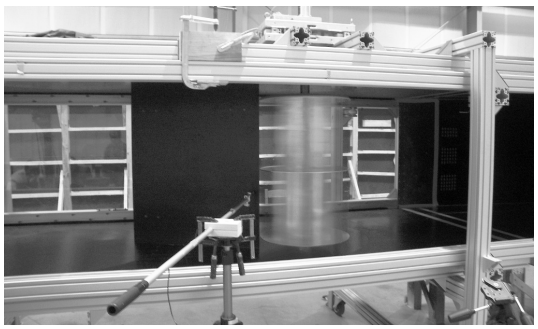

Figure 2: Experimental setup.

2.2 Results

The experimental setup is shown in figure 2. This figure presents the test section of the closed return wind tunnel with one side of the section open. The two-stage Savonius rotor equipped with an adjustable stator is visible. A pitot tube located at the inlet to the test section is utilised in order to determine the wind speed. Furthermore, the rotational speed of the rotor and the torque acting on the shaft are also measured.

The wind tunnel can attain maximal velocity of about $50\,\mathrm{m\,s^{-1}}$. Experimental results for $U \approx 10\,\mathrm{m\,s^{-1}}$ are shown in figures 3 and 4. Three different configurations are discussed here, namely the classic Savonius design and the innovative design equipped with a stator at 40° and 60° angle of attack. Figure 3 presents the power C_P and figure 4 torque coefficient C_T distributions as a function of tip speed ratios λ. In order to indicate the uncertainty in measurements absolute errors are superimposed.

Figure 4 shows that the torque coefficient distributions of the modified design are lower in comparison with the original Savonius wind turbine even that the higher torques acting on a shaft. This may be explained by the larger active surface area HD for the modified design in equation (2). Furthermore, the effect of larger active surface area HD can is compensated by the same stator directing the flow and generating higher torques. Figure 3 shows the distribution of C_P as a function of λ. The larger the stator angle of atack the higher the efficiency. Obviously, the innovative design with the stator at 40° and 60° is always more efficient for the same wind speed $\sim 10\,\mathrm{m\,s^{-1}}$. This shows that even for low wind speeds the innovative design if more efficient and may be regarded as an advantage of the proposed design over the Savonius wind turbine.

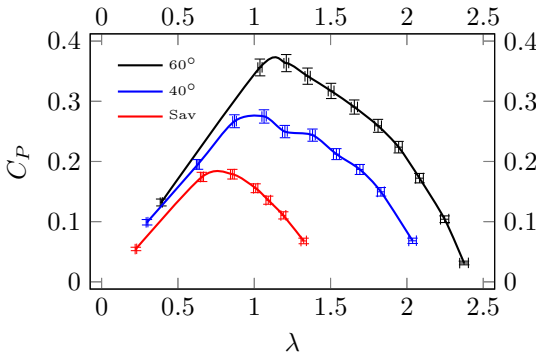

Figure 3: C_P distribution as a function of λ.

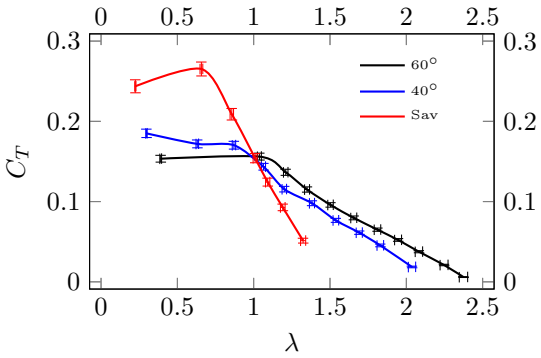

Figure 4: C_T distribution as a function of λ.

3 NUMERICAL CALCULATIONS

3.1 Governing equations

The numerical calculations have been performed by means of CFD. The turbulent flow of air is regarded as an incompressible medium. RANS approach has been utilised in order to model the turbulence, namely the two-equation Shear Stress Transport turbulence model [8]. The average form of mass conservation equation has the form

$$\nabla \cdot \bar{\mathbf{U}} = 0. \tag{5}$$

The Reynolds equation is

$$\rho \frac{\mathrm{d}\bar{\mathbf{U}}}{\mathrm{d}t} = \rho \vec{g} - \nabla p_e + \nabla \cdot \left(2\mu_t \bar{\mathbf{D}}\right), \tag{6}$$

where the effective pressure $p_e := \langle p \rangle + 2/3\rho k$ and the effective viscosity consists of the eddy and molecular components $\mu_e := \mu_t + \mu$. Two additional transport equations are those for modelled kinetic energy of velocity fluctuation which arises from Reynolds stress transport equation

$$\rho \frac{\mathrm{d}k}{\mathrm{d}t} = 2\mu_t \bar{\mathbf{D}}^2 + \nabla \cdot \left(\left(\frac{\mu_t}{\sigma_{k3}} + \mu \right) \nabla k \right) - C_\mu \rho k \omega \tag{7}$$

and the turbulent frequency ω. This is analogous to k transport

$$\rho \frac{\mathrm{d}\omega}{\mathrm{d}t} = \alpha_3 \frac{\omega}{k} 2\mu_t \bar{\mathbf{D}}^2 + \nabla \cdot \left(\left(\frac{\mu_t}{\sigma_{\omega 3}} + \mu \right) \nabla \omega \right) - \beta_3 \rho \omega^2 + (1 - F_1) \frac{2}{\omega} \rho \sigma_{\omega 3} \nabla k \cdot \nabla \omega. \tag{8}$$

The eddy viscosity is defined as $\mu_t = \rho k \omega^{-1}$. Constants marked with the subscript 3, namely σ_{k3}, $\sigma_{\omega 3}$, α_3, β_3 are linear combinations of constants from the component models.

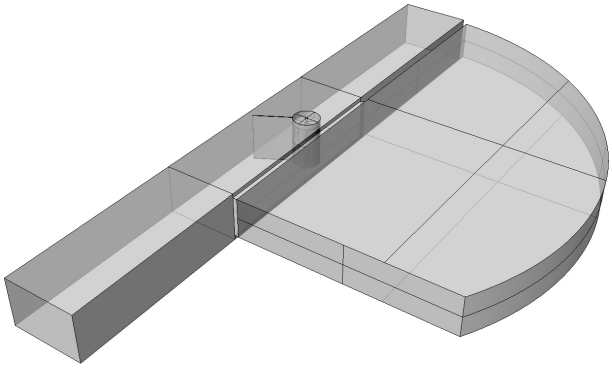

Figure 5: Flow domain.

3.2 Boundary conditions and mesh

The flow domain resembles a wind tunnel with one side partially open to the atmosphere as shown if figure 5. It is divided into parts merged by means of interfaces. These include the rotating rotor and the steady wind tunnel and surrounding area. The boundary conditions selected here include tunnel inlet with a prescribed velocity $10.5\,\mathrm{m\,s^{-1}}$ and medium turbulent intensity conditions. Furthermore, the so called 'far field' condition is chosen with prescribed constant atmospheric pressure. The surrounding area is limited by symmetry planes and wind tunnel walls are modelled as no slip wall. The same concerns the rotor. The only difference being the rotating frame of reference.

The domains have an unstructured grid consisting of mostly tetrahedral elements. The total number of elements covering the flow area is about 9 million. In order to properly resolve flow near the wall special elements around the blades are generated. The wall function approach has been used to provide near wall boundary conditions for the mean flow. The average value of y^+ distribution does not exceed 2 for all the time steps. Finally, the time step of the transient calculations corresponds to 4° of revolution and the angular velocity of the rotor corresponds to 4 revolutions per second.

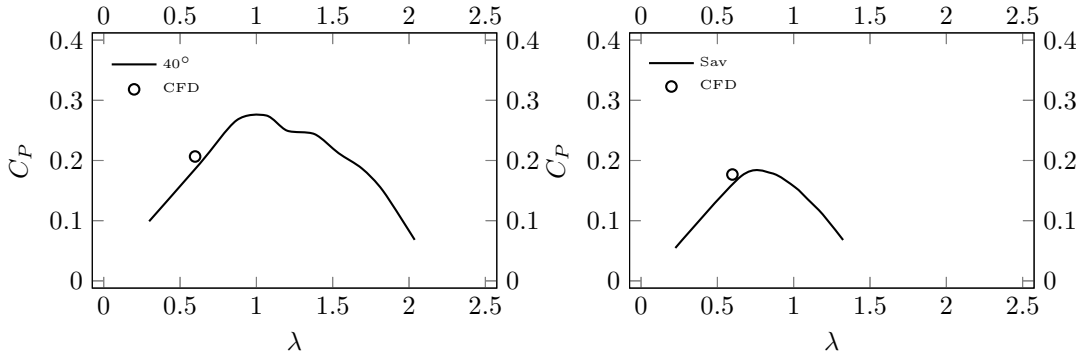

Figure 6: Experiment vs numerical prediction.

3.3 Results of calculations

Figures 6 show the experimental values of C_P versus CFD calculations for two selected designs as a function of λ. These include the classic Savonius rotor and the innovative design equipped with a stator at 40° angle of attack. Circles correspond to the numerical prediction. Good agreement is visible.

Figures 7 present the torque coefficient C_T distribution as a function of revolution angle α for three different configurations, namely Savonius rotor and an innovative design equipped with a stator at 40° and 60° angle of attack. These are results of transient calculations. The four peaks per curve are visible due to the two rotors rotated by an angle relative to each other. The torque coefficient distributions of the modified design are lower in comparison with the original Savonius wind turbine. This is because the presence of the stator increases the active surface area HD.

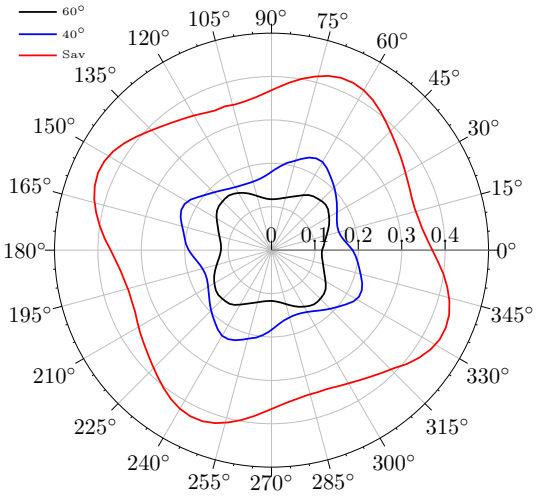

Figure 7: C_T distribution as a function of the angular position of the rotor α.

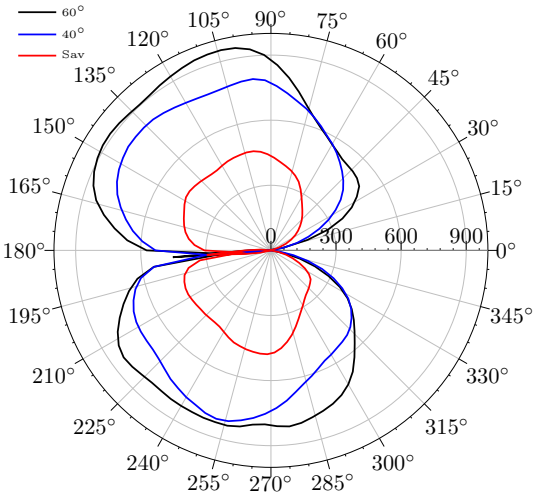

Figure 8: Λ_2 distribution as a function of the angular position of the rotor α.

4 COMPARISON CRITERIA

The proposed criteria allow for evaluation and comparison of various designs and solutions. Invariants of velocity gradient tensors $\nabla\mathbf{U}$, or its decomposition

$$\nabla\mathbf{U} = \mathbf{D} + \mathbf{A} \tag{9}$$

are often used [3] in turbulence modelling. This is because they contain all the necessary information that are responsible for kinetic energy dissipation and vortex stretching [13]. In the above equation $\mathbf{D}$ is the rate-of-strain tensor and $\mathbf{A}$ represents the spin (vorticity) tensor.

The vorticity measure $\mathcal{Q}$, firstly investigated in [4], is defined by means of the integral of the velocity gradient tensor second invariant in the following form

$$\mathcal{Q} = \iiint_V \mathrm{tr}\,(\nabla\mathbf{U})^2\,\mathrm{d}V = \iiint_V \left(\mathrm{tr}\mathbf{D}^2 - \|\mathbf{A}\|^2\right)\mathrm{d}V. \tag{10}$$

The above criterion represents a global balance between the power of energy dissipation N_d and

vortex structures by means of the vorticity magnitude or enstrophy $\mathcal{E}^*$

$$\mathcal{Q} = \frac{N_d}{2\mu} - \mathcal{E}^*. \tag{11}$$

These structures are generated by the rotor and may affect the efficiency [12]. Another criterion λ_2 [5] is investigated in this paper. The vorticity measure Λ_2 is defined by means of the integral of the λ_2 in the following form

$$\Lambda_2 = \iiint_V \lambda_2 \left(\mathbf{D}^2 + \mathbf{A}^2\right) \mathrm{d}V \tag{12}$$

where $\lambda_2(\mathbf{D}^2 + \mathbf{A}^2)$ represents the second ordered eigenvalue of tensor $\mathbf{D}^2 + \mathbf{A}^2$. The three eigenvalues are ordered as follows $\lambda_1 \geq \lambda_2 \geq \lambda_3$.

Figure 8 shows the distribution of the vorticity measure Λ_2 defined by means of equation (12) which can be used to compare various designs. The higher the efficiency the higher the values of Λ_2. Equation (12) is appropriate for individual time steps, while for the total revolution it is necessary to use the time average of Λ_2 instead

$$\langle \Lambda_2 \rangle = \frac{1}{\Delta t} \int_t^{t+\Delta t} \Lambda_2 \, \mathrm{d}t. \tag{13}$$

The above time integral (13) can be used directly to evaluate specific turbine in terms of a vorticity measure. This is summarised in table 1 where the ratio of $\langle \Lambda_2 \rangle$ to $\langle \Lambda_{2S} \rangle$ of the respective Savonius design is listed. It follows previous observations and makes it possible to anticipate a relationship between vorticity measure and efficiency of a turbine.

Cinfiguration	$\langle \Lambda_2 \rangle / \langle \Lambda_{2S} \rangle$
Savonius	1.000
40°	2.543
60°	2.834

Table 1: $\langle \Lambda_2 \rangle / \langle \Lambda_{2S} \rangle$ values for different configurations.

5 CONCLUSIONS

Conclusions can be summarised in the following points:

- Usually, all data presented on the numerical aspect in the available literature are mostly two-dimensional and steady state. A three dimensional numerical analysis of the transient phenomena occurring in the innovative turbine is investigated here.
- Wind tunnel experiments prove that the innovative modification of the classic Savonius shows higher efficiency for the same wind speed.
- The increased efficiency is due to presence of the stator which directs the air and makes it possible to take better advantage of its energy.

- A relationship between vorticity measure and efficiency of a turbine can be anticipated. The proposed criteria are related to the vortex structures being generated by the rotor and affecting pressure distribution around it and thus the performance. The time integral of this measures can be used directly to evaluate specific turbine.

REFERENCES

[1] B.F. Blackwell, R.E. Sheldahl, L.V. Feltz, Wind Tunnel Performance Data for Two- and Three-Bucket Savonius Rotor, *Sandia Laboratories Report SAND 76-0131*, **105**, 1977.

[2] P. Doerffer, *International patent application PCT/PL2012/000125 and national patent application*

[3] G. Haller, An objective definition of a vortex. *Journal of Fluid Mechanics*, **525**, 1–26, 2005.

[4] J. C. R. Hunt, A. Wray, P. Moin, Eddies, stream, and convergence zones in turbulent flows. *Center for Turbulence Research Report CTR-S88*, 1988.

[5] J. Jeong, F. Hussain, On the identification of a vortex. *Journal of Fluid Mechanics*, **285**, 69–94, 1995.

[6] M.A. Kamoji, S.B. Kedare, S.V. Prabhu, Experimental investigations on single stage, two stage and three stage conventional Savonius rotor, *International Journal of Energy Research*, **32**, 877–895, 2008.

[7] J. Menet, Prediction of the aerodynamics of a new type of vertical axis wind turbine: the reverse bladed rotor. In: *Proc. of the European Wind Energy Conference*, 2008.

[8] F. R. Menter, Two-Equation Eddy-Viscosity Turbulence Models for Engineering Applications, *AIAA Journal*, **32** 8, 1598–1605, 1994.

[9] M.H. Mohamed, G. Janiga, E. Pap, D. Thevenin, Optimisation of Savonius turbines using an obstacle shielding the returning blade, *Renewable Energy*, **35**, 2618–2626, 2010.

[10] M. Nakajima, S. Iio, T. Ikeda, Performance of Double-Step Savonius Rotor for Environmentally Friendly Hydraulic Turbine, *Journal of Fluid Science and Technology*, **3**, 410–419, 2008.

[11] U.K. Saha, S. Thotla, D. Maity, Optimum design configuration of Savonius rotor through wind tunnel experiments, *Journal of Wind Engineering and Industrial Aerodynamics*, **96**, 1359–1375, 2008.

[12] K. Tesch, K. Kludzinska, P. Doerffer, Investigation of the Aerodynamics of an Innovative Vertical-Axis Wind Turbine. *Flow, Turbulence and Combustion*, **95** 4, 739–754, 2015.

[13] K. Tesch, On invariants of fluid mechanics tensors. *Task Quarterly* **17** 3–4, 1000–1008, 2013.